Applied Catalysis B: Environmental 179 (2015) 583–588

Contents lists available at ScienceDirect

Applied Catalysis B: Environmental

journal homepage: www.elsevier.com/locate/apcatb

Visible light activation photocatalytic performance of PbSe quantum dot sensitized TiO_2 Nanowires

Zoltán Győri [a], Zoltán Kónya [b,c], Ákos Kukovecz [a,b,*]

[a] MTA-SZTE "Lendület" Porous Nanocomposites Research Group, Rerrich Béla tér 1., Szeged H-6720, Hungary
[b] Department of Applied and Environmental Chemistry, University of Szeged, Rerrich Béla tér 1., Szeged H-6720, Hungary
[c] MTA-SZTE Reaction Kinetics and Surface Chemistry Research Group, Rerrich Béla tér 1., Szeged H-6720, Hungary

ARTICLE INFO

Article history:
Received 13 February 2015
Received in revised form 19 May 2015
Accepted 29 May 2015
Available online 9 June 2015

Keywords:
PbSe
quantum dots
TiO_2
nanowires
photosensitization

ABSTRACT

In this paper we describe the use of differently sized PbSe quantum dots as photosensitizers for anatase TiO_2 nanowires under visible light illumination. After the organometallic synthesis of PbSe quantum dots with three different average diameters (1.8, 2.5 and 4.7 nm), the nanocrystals were attached to the surface of nanowires with thioglycolic acid as a linker molecule. These quantum dot decorated nanowires were used as photocatalyst in the methyl orange degradation model reaction with promising results. The best performance achieved was 90% degradation of the initial concentration of methyl orange in six hours over 2.5 nm PbSe quantum dot sensitized nanowires using a 40 W quartz UV lamp equipped with a 400 nm cut-off filter.

1. Introduction

TiO_2 is one of the most efficient photovoltaic materials and photocatalysts [1–3]. It is relatively cheap and stable, has high oxidative power and poses only minimal environmental hazards. With current research trends moving into the nanoscale regime, one-dimensional (1D) nanostructured TiO_2 materials including nanowires, nanofibers, nanorods and nanotubes have become popular recently. These 1D TiO_2 materials are more easily separated and recovered from a heterogeneous catalytic system than isotropic TiO_2 nanoparticles because of their large aspect ratio and micrometer sized length [4–6]. Nevertheless, 1D TiO_2 materials maintain the favorable properties of nanomaterials, e.g. high specific surface area [7]. Although quantum confinement in TiO_2 occurs only below 50 nm [8,9], surface states related to the large specific surface area as well as states caused by impurities and defects could alter the band structure of 1D TiO_2 materials.

The main issue with the photocatalytically most active anatase phase TiO_2 is its relatively large band gap (3.2 eV) that limits its organic chemical degradation performance to UV irradiation only. Since the largest proportion of the incident radiation from the Sun to the Earth is in the visible and infrared range, it is reasonable to attempt activating TiO_2 for this region as well. There are several strategies for photosensitization to extend the absorption window of the different TiO_2 based photovoltaics and photocatalysts to the visible range [10–12]. One of these methods is sensitization with organic dyes or semiconductor nanocrystals such as quantum dots (QDs) [13–15]. QDs offer numerous advantages over organic dyes, e.g. broader absorption profile with tunable absorption window and excellent resistance against photobeaching. There are many examples in the literature for using QDs as photosensitizers in the field of solar cells [16,17] or in photocatalysts under visible light irradiation [16–20]. QDs studied so far as sensitizers are mostly CdSe [16–19,21,22], CdS [20,23–26], CdTe [27], InPand InAs [27], PbS [21,28,29] and PbSe [22,30].

The most attractive property of quantum dots is their size dependent optical and electronic behavior, which is the consequence of the quantum confinement of the electrons and holes in the QDs. Lead chalcogenide nanocrystals (PbS, PbSe and PbTe) are more beneficial than the widely used cadmium-based systems because of their large Bohr exciton radius (20-46 nm versus 4-10 nm in the case of cadmium chalcogenides), which allows their fabrication with extremely strong quantum confinement [31]. The first and most dramatic indication of carrier multiplication has also been obtained on lead-chalcogenide QDs [32]. Furthermore, lead chalcogenide QDs could emit in the near-infrared region, which

* Corresponding author.
E-mail address: kakos@chem.u-szeged.hu (Á. Kukovecz).

http://dx.doi.org/10.1016/j.apcatb.2015.05.056
0926-3373/

makes them also ideal material in biological imaging and labeling [33,34] and due to their high nonlinearities they also can be used as optical switches [34].

While numerous works are available in the literature about different cadmium chalcogenide QD sensitized TiO_2 structures and their uses in solar cells or in photocatalytic reactions, considerably less papers discuss lead chalcogenides, especially PbSe QDs and their utilization in photocatalysis. To the best of our knowledge, the use of PbSe QD sensitized anatase TiO_2 nanowires in a photocatalytic model reaction is reported here for the first time.

2. Experimental

2.1. Chemicals

PbO (99.9%, Sigma-Aldrich), Se (99.99%, Sigma-Aldrich), trioctylphosphine (TOP, 90%, Sigma-Aldrich), oleic acid (OA, 90% Sigma-Aldrich), octadecene (ODE, 90%, Sigma-Aldrich), thioglycolic acid (TGA, 98%, Sigma-Aldrich), acetonitrile (99%, Reanal), tetrachloroethylene (99.9%, Sigma-Aldrich), anatase TiO_2 powder (99.8%, Sigma-Aldrich), TiO_2 nanopowder (Degussa, P25), sodium hydroxide (99.5%, Molar Chemicals Kft.). All chemicals were used as received.

2.2. Synthesis of PbSe nanocrystals

The PbSe QDs were synthesized in a noncoordinating solvent by a modified method adapted from the earlier work of Yu and coworkers [35]. 2.0 mmol PbO was dissolved in 1.5 mL OA with 10 mL ODE and heated to 180 °C in inert atmosphere. The selenium stock solution contained 4.0 mmol Se dissolved in 2 mL TOP. The crystal growth temperature was 150 °C and after the desired crystal growth time (5, 10 and 15 s) the reaction was quenched immediately by injecting 10 mL cold octadecene to the synthesis mixture. The resulting nanocrystals were purified by repeated extractions and precipitations.

2.3. Synthesis of TiO_2 nanowires (NWs) with anatase crystal structure

The synthesis was based on the hydrothermal recrystallization of TiO_2 as described earlier by Horváth et al. [36]. In a typical synthesis 50 g anatase TiO_2 powder was placed into an autoclave with 1 L 10 M NaOH solution. The autoclave was maintained at 185 °C for 24 h while it was rotated continuously around its short axis at 28 rpm. The autoclave was subsequently cooled to room temperature and the formed $Na_2Ti_3O_7$ nanowires were washed with dilute HCl aqueous solution and distilled water to pH 7. $Na_2Ti_3O_7$ nanotubes (NTs) used as reference material in the photocatalytic experiment were synthesized with a similar method, but the initial amount of anatase TiO_2 powder was 250 g and the autoclave was maintained at 155 °C and rotated with 3 rpm. These NTs were washed only with distilled water.

The resulting $H_2Ti_3O_7$ nanowires were filtered on a glass filter and heat-treated at 700 °C for 24 h to convert the material into anatase while maintaining the nanowire morphology. Reference $Na_2Ti_3O_7$ nanotubes were not heat treated.

2.4. Anchoring the QDs onto the surface of the nanowires

Thyoglicolic acid was used to anchor the QDs onto the TiO_2 surface. The NWs were treated in 1 M TGA-acetonitrile solution for 24 h then filtered and washed with acetonitrile and toluene. Then 90 mg of these TGA-functionalized NWs were stirred intensely for 48 h in suspensions containg different sized PbSe QDs. Thereafter, the nanowires were filtered on a membrane filter and washed with toluene.

2.5. Methyl orange degradation test reaction

In the methyl orange degradation reaction 10 mg of photosensitized NWs were sonicated for 30 min in the dark in 10 mL methyl orange (MO) solution with 9.6 mg/L concentration to establish adsorption equilibrium. The MO-nanowire suspensions were then irradiated by visible light under vigorous stirring by placing a 40W quartz UV-lamp equipped with a 400 nm cut-off filter 12 cm above the reaction vessel. After a preset reaction time the suspension was centrifuged for 15 minutes at 3200 rpm, the UV–vis absorbance spectrum of the supernatant was recorded and the concentration of the remaining MO was calculated from the absorbance at λ = 462 nm.

2.6. Sample Characterization

Transmission Electron Microscopy (TEM) measurements were done on Philips CM10 and FEI Tecnai G^2 F20 X-Twin microscopes. UV-VIS absorbance and reflectance spectra were recorded on an Ocean Optics USB4000 spectrometer using a DH-2000-BAL UV-Vis-NIR light source and MgO reflectance reference. The NIR absorbance spectrum of PbSe with 4.7 nm mean diameter was recorded with a Thermo Scientific Antaris II FT-NIR Analyzer. The absorbance measurements were carried out in tetrachloroethylene solution. The crystal structure of the synthesized QDs was analyzed by powder X-ray Diffraction (XRD) on a RigakuMiniFlex II system operating with Cu Kα radiation. Energy Dispersive X-ray spectroscopy (EDS) measurements were performed in a Hitachi S-4700 SEM Cold Field Emission Scanning Electron Microscope (SEM) equipped with a Röntec QX2 spectrometer. Brunauer-Emmett-Teller (BET) specific surface area measurements were performed on a Quantachrome NOVA 3000e surface area & pore size analyzer.

3. Results and discussion

TEM images of the synthesized PbSe nanocrystals are presented in Fig. 1. The nanocrystals exhibited monodisperse shape and size distribution. The average diameter of the nanocrystals was 1.8 ± 0.4 nm (std. dev.: 18%), 2.5 ± 0.5 nm (std. dev.: 15%) and 4.7 ± 0.6 nm (std. dev.: 10%) after 5, 10 and 15 s sampling time, respectively.The XRD patterns of the PbSe nanocrystals are shown in Fig 1D and the characteristic reflections of bulk cubic PbSe are marked at the bottom of the graph for reference. The average QD diameters were also estimated from XRD peak broadening using the Scherrer equation as 1.2 nm, 1.6 nm and 2.8 nm after 5, 10 and 15 s synthesis time, respectively. Observing broadened weak reflections similar to those in Fig 1D is rather common in the literature of very small quantum dots [37–41].

The optical absorption spectra of the QDs are presented in Fig. 2. The values of the first excitonic absorption peaks with increasing diameter were 698, 780 and 1198 nm respectively. These values are in good agreement with Sashchiuk et al.'s observations [42]. However, slightly different data about the positions of the first absorption peaks of different sized PbSe QDs can be found in the literature as well. Evans at al. [43] observed absorption peaks at 690 and 750 nm for smaller sized (1.2 and 1.4 nm) PbSe QDs, while Yu et al. [35] measured about 1400 nm peak maxima for about 4.5 nm sized QDs.

The anatase TiO_2 NWs were obtained from $H_2Ti_3O_7$ nanowires after washing and calcining them at 700 °C. TEM and SEM images of the TiO_2 nanowires confirm that the anisotropic morphology was preserved after the 24 hours of heat treatment (Fig. S1.) and the remaining Na impurity was negligible (below 0.2 wt %, see Fig. S2.).

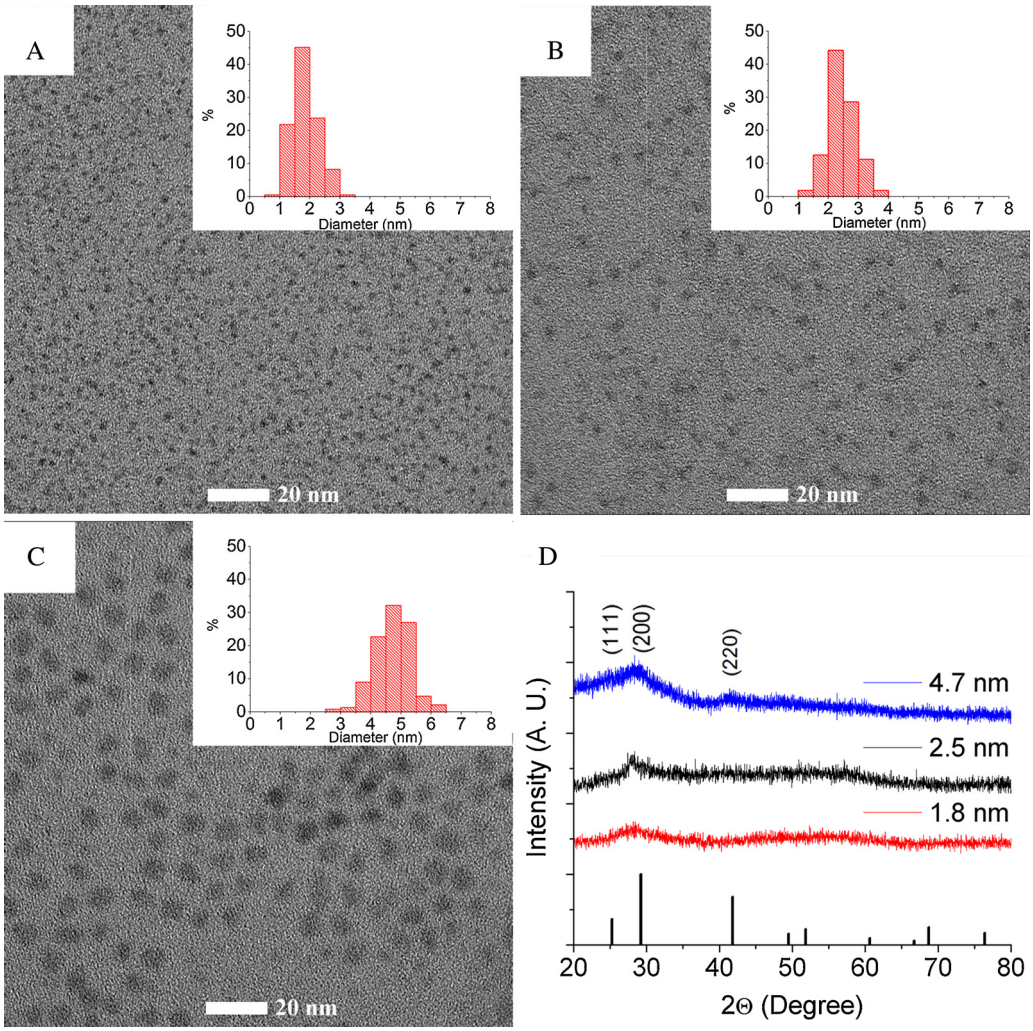

Fig. 1. Transmission electronmicroscopy images of the PbSe QDs samples. (A) 1.8 nm, (B) 2.5 nm (C) with 4.7 nm mean diameter and XRD profiles of the PbSe QDs (D).

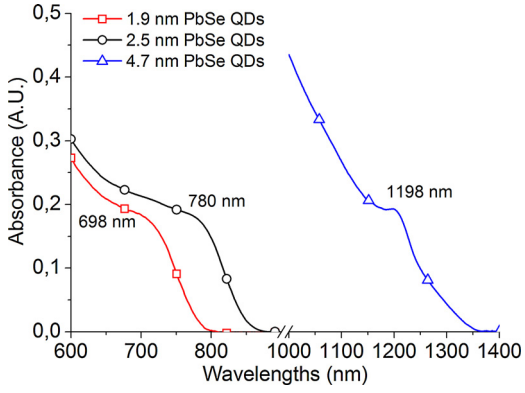

Fig. 2. UV-Vis-NIR absorption spectra of the PbSe QDs samples

These NWs measured 1.4 ± 0.9 μm in length and 81.3 ± 38.1 nm in diameter. The XRD patterns of the as-synthesized titanate NWs as well as those of the calcined TiO_2 NWs are shownin Fig. S3. The presence of the anatase crystalline phase required for efficient photocatalysis is confirmed in the calcined sample.

The obtained white anatase nanowires were treated with TGA and then decorated with clear PbSe QD sols as described above. The successful linking of the QDs to the nanowires was indicated by the change of the color of the washed and filtered product to pale brown. Fig. S4. depicts the reflectance spectra of the pristine and QDs sensitized NWs. It can be seen in Fig. S4. that the reflectance of the PbSe-decorated NWs is 20-25% smaller than that of the untreated ones in the whole visible and NIR region. Hence these sensitized nanowires can absorb more light than the untreated ones.

Fig. 3. shows the transmission electron micrographs of TiO_2 NWs sensitized with 1.8 nm (A), 2.5 nm (B) and 4.7 nm (C) PbSe QDs. The nanocrystals can be seen clearly on the surface of the nanowires. PbSe QD reflections cannot be identified in the corresponding XRD profiles (Fig. 2D) because of the low concentration of the quantum dots. The TEM image of the PbSe QD decorated $Na_2Ti_3O_7$ nanotubes (used as reference material) is depicted in Fig. S5 along with the corresponding EDS and XRD data in Fig S6.

To investigate the photosenzitization performance of the different sized QDs on the nanowires, methyl orange (MO) degradation model reactions were performed in visible light illumination. The light source was a 40 W quartz UV lamp with a 400 nm cut off filter; the irradiance spectrum of the light source is depicted in the Supplementary Informations in Fig S7. Since wavelengths shorter than 400 nm were cut off, any MO degradation can be attributed to the succesful electron injection from the sensitizer QDs into the conduction band of the NWs (Fig. 4).

The MO suspensions were centrifugated after the preset visible-light irradiation periods and the concentration of the remaining MO was calculated from the λ=462 nm absorbance value of super-

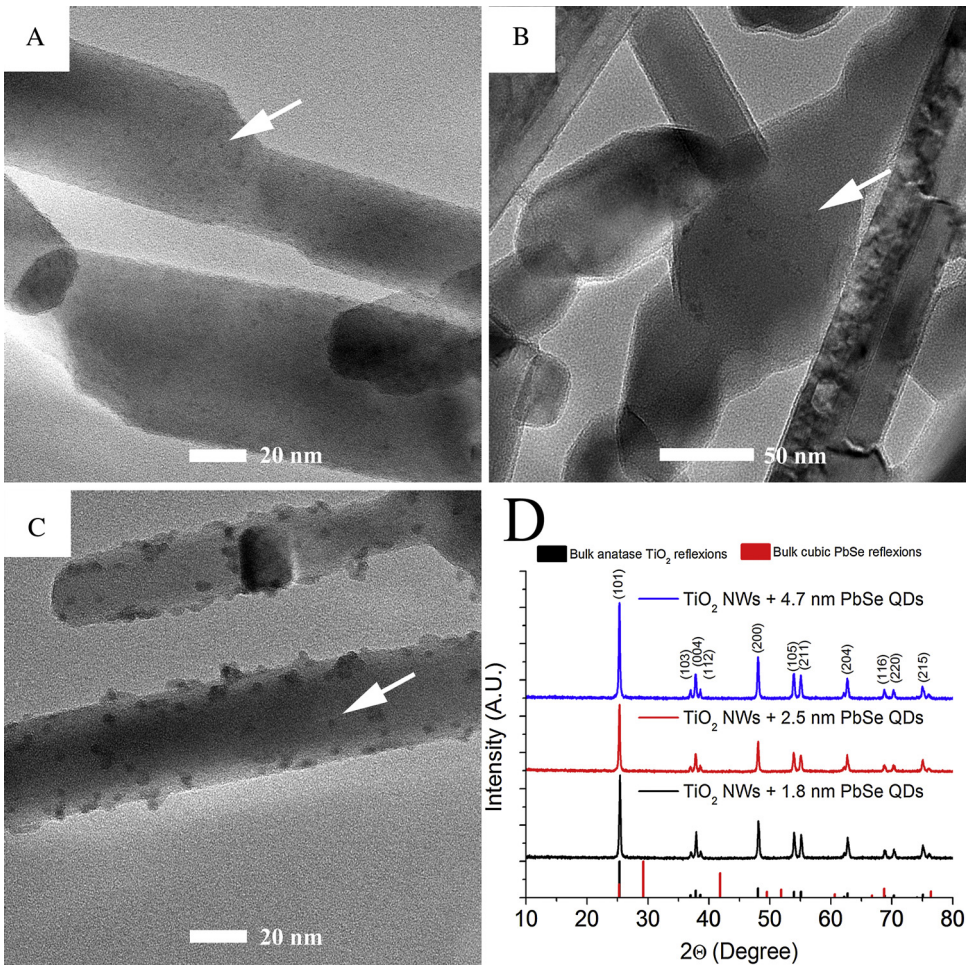

Fig. 3. TEM images of the sensitized nanowires with 1.8 nm (A), 2.5 nm (B) 4.7 nm (C) PbSe QDs and XRD diffractograms of the QDs photosensitized NWs (D).

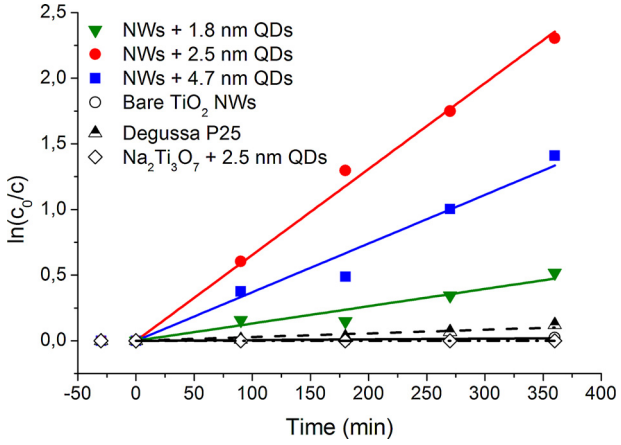

Fig. 4. Linearized kinetic plots of the methyl orange degradation by different sized PbSe QDs sensitized TiO_2 nanowires under visible light irradiation.

natants. Photodegradation efficiency calculations were corrected by the equilibrium amount of methyl orange adsorbed on the surface of TiO_2 nanowires (60 mg/g) or P25 (30 mg/g). With the cut-off filter in place, bare TiO_2 NWs and P25 showed minimal catalytic activity, while PbSe photosensitized nanowires offered appreciable performance as demonstrated by the linearized kinetic plots in Fig. 3. The photocatalityc activity of the sensitizer PbSe QDs also investigated on inert support: PbSe QDs with 2.5 nm mean diameter were attached to $Na_2Ti_3O_7$ nanotubes, as later studies on such nanotubes have indicated that neither as-prepared nor acid treated nanotubes exhibit any photocatalytic activity [44]. In our experiments neither the pristine nanotubes nor those decorated with PbSe QDs (3.33 wt% PbSe) exhibited any detectable photocatalityc activity under visible light irradiance. This confirms that PbSe QDs in the anatase nanowire + PbSe QD system act only as photosensitizers and not as a standalone photocatalyst.

Nanowires decorated with 2.5 nm PbSe QDs converted 90.0% of the initial amount of MO after 6 hours of irradiation. Those sensitized with 4.7 nm QDs and 1.8 nm QDs offered 75.6% and 40.4% MO degradation performance, respectively.

In order to interpret these data, we measured the PbSe content of the catalysts by EDS, the specific surface area of the anatase nanowires by nitrogen adsorption (100 m^2/g as calculated by the BET method) and considered the quantum dots to be spherical and monodisperse. In fractional coverage calculations the apparent area of the QDs was estimated as that of a circle with identical diameter. Table 1. summarizes these derivative values for 6 hours of reaction time.

The TiO_2-catalyzed photodegradation of dyes follows the Langmuir-Hinshelwood kinetics, which can be simplified to apparent fist-order kinetics at low dye concentrations. It can be described with the $\ln(c_0/c)=k_{app}t$ equation, where c is the concentration of the dye at time t, c_0 is the initial dye concentration and k_{app} is the apparent reaction rate constant. The apparent reaction rate constants of sensitized NWs are also shown in Table 1. While undecorated anatase nanowires exhibited minimal catalytic activity ($k_{app} = 0.0541\times10^{-3} \pm 0.0191\times10^{-3}$) under visible light

Table 1
PbSe weight ratio, particle concentration, fractional coverage, QD surface area, MO degradation and k_{app} values calculated for PbSe decorated anatase nanowires.

	PbSe QDs weight ratio (%)	Particle concentration ($x10^{10}$ particles*cm^{-2})	Fractional coverage	Calculated QD surface area (m^2/g)	MO degradation after 6 hours (%)	k_{app} ($x10^{-3}$ (min^{-1})
1.8 nm PbSe + NWs	2.88	126.3	0.032	6.5	40.4	1.32 ± 0107
2.5 nm PbSe + NWs	2.34	38.3	0.019	3.8	90.0	6.54 ± 0133
4.7 nm PbSe + NWs	2.75	6.8	0.012	2.4	75.6	3.71 ± 0.202

irradiation, the highest achievable degradation rate (on 2.5 nm QDs sensitized NWs) was over x120 higher with $k_{app} = 6.54 \times 10^{-3} \pm 0135 \times 10^{-3}$. Moreover, nanowires photosensitized with 2.5 nm QDs have exhibited x23 higher k_{app} value than a Degussa P25 TiO_2 sample under the same illumination conditions ($k_{app} = 2.81 \times 10^{-4} \pm 0{,}0345 \times 10^{-5}$). Comparing further the apparent rate constant of the 2.5 nm PbSe sensitized NWs to undecorated nanowires of similar dimensions [45], it turns out that anatase TiO_2 NWs have only 11.9 times higher activity under UV illumination (k_{app} = 0.078 ± 0.003) than the 2.5 nm PbSe QDs sensitized NWs under visible light.

Though the photosensitized NWs were decorated with similar amounts of different sized PbSe QDs in all three cases, the effect of the QDs size on the reaction rate of methyl orange degradation is not monotonic. Smaller sized QDs have wider band gap, thus they are expected to have favourable conduction band energies for injecting electrons into TiO_2 at a higher rate. Larger sized QDs with smaller band gaps could be excited easier and may have higher light absorption capability across their smaller surface curvature. We assume that there is an optimum size for the sensitizer QDs when the overall effect of the different factors is the most favorable. QDs with 2.5 nm diameter appear to be the closest to this optimum size amongst the investigated PbSe QDs. Some reports available in the literature discuss a similar trend on cadmium chalcogenide QDs. Kongkanand et al. [16] investigated the power conversion efficiency on TiO_2 films sensitized with CdSe QDs between 2.2 and 3.7 nm diameter and observed maximum efficiency in the case of 3.0 nm CdSe QDs. Prabakar et al. also reported size dependent charge injection from CdSe QDs into dye co-sensitized mesoporous TiO_2 solar cells. The photoconversion efficiencies for small and larg particle size QD solar cells were lower and they observed maximum power conversion efficiency when using intermediate sized 3.3 nm diameter CdSe QDs co-sensitized solar cells [46].

The overall visual light activated photocatalytic performance of the 2.5 nm PbSe QD sensitized TiO_2 nanowires (90% MO degradation in 6 hours at 40 W total illumination) compares very favorably with literature results. Wang et al. [22] demonstrated on heterostructured thin film catalysts consisting of PbSe nanocrystals and layer-by-layer deposited TiO_x that the larger (~7 nm) diameter PbSe nanocrystals produced noticeable photobleach under visible light. W. Ho and co-workers [18] synthesized CdSe photosensitized TiO_2 nanoparticles with a sonochemical method and the photocatalytic activities were measured by 4-chlorophenol degradation with a 300 W tungsten halogen lamp with 400 nm cut-off filter. 200 mg photocatalyst was suspended in 200 mL 2.5×10^{-4} mol/L 4-chlorophenol aqueous solution. The sensitized catalyst reduced the initial 4-chlorophenol concentration by 32% after 8 hours of irradiation. Lim and co-workers [19] synthesized a CdSe-TiO_2 photocatalyst with the solvothermal method. Their photocatalytic activity measurements were performed with 50 mg catalyst in 50 mL 1×10^{-6} mol/L methylene blue solution with a λ=420 nm visible- and λ=365 nm UV-light source with 8 W output. They observed 42% degradation in visible light and 59% in UV-light after 4 hours of illumination. Zhu et al. [20] sensitized TiO_2 nanotubes with CdS nanocrystals and these NTs were able to reduce the initial methylene blue concentration by 83.7% with a 150 W xenon arc lamp after 6 hours of irradiation (50 mg catalyst and 100 mL 20 mg/L methylene blue solution). L. Mao and co-workerssensitized 20 nm TiO_2 nanoparticles with CdS QDs. These NPs degraded 92.2% of the Rhodamine B model compound after 60 min under 160 W high pressure mercury lamp irradiation used with a 400 nm cut-off filter (25 mg catalyst, and 100 mL 60 mg/L Rhodamine B solution) [47]. Even though these results are not directly comparable with ours, they indicate that the photocatalytic activity of PbSe QD sensitized TiO_2 nanowires under visible light irradiation is remarkable.

4. Conclusion

Organometallically synthesized PbSe quantum dots attached to the surface of the anatase TiO_2 nanowires by thioglycolic acid linker are efficient photosensitizers for the visible spectral range. Titania samples decorated with PbSe QDs of 2.5 nm mean diameter could reduce the initial methyl orange concentration by 90% in 6 hours when illuminated by λ>400 nm visible light. PbSe QDs with 2.5 nm mean diameter appear to be the closest to the overall optimum size with respect to the photosensitizing effect. Samples decorated with PbSe QDs smaller or larger than 2.5 nm did not perform so well, nevertheless, every PbSe sensitized titania nanowire photocatalyst has outperformed P25 by at least a factor of five.

Acknowledgement

The financial support of the Hungarian National Research Fund projects OTKA NN 110676 and K 112531 is acknowledged.

Appendix A. Supplementary data

Supplementary data associated with this article can be found, in the online version, at http://dx.doi.org/10.1016/j.apcatb.2015.05.057

References

[1] A.L. Linsebigler, G.Q. Lu, J.T. Yates, Photocatalysis on TiO_2 Surfaces - Principles, Mechanisms, and Selected Results, Chemical Reviews 95 (1995) 735–758.
[2] J.-F. Lin, W.-C. Yen, C.-Y. Chang, Y.-F. Chen, W.-F. Su, Enhancing organic-inorganic hybrid solar cell efficiency using rod-coil diblock polymer additive, Journal of Materials Chemistry A 1 (2013) 665–670.
[3] C.-S. Tsao, C.-M. Chuang, C.-Y. Chen, Y.-C. Huang, H.-C. Cha, F.-H. Hsu, C.-Y. Chen, Y.-C. Tu, W.-F. Su, Reaction Kinetics and Formation Mechanism of TiO_2 Nanorods in Solution: An Insight into Oriented Attachment, Journal of Physical Chemistry C 118 (2014) 26332–26340.
[4] P. Pattanaik, M.K. Sahoo, TiO_2 photocatalysis: progress from fundamentals to modification technology, Desalination and Water Treatment, 52 (2014) 6567-6590.
[5] A.-R. Rautio, P. Maki-Arvela, A. Aho, K. Eranen, K. Kordas, Chemoselective hydrogenation of citral by Pt and Pt-Sn catalysts supported on TiO_2 nanoparticles and nanowires, Catalysis Today 241 (2015) 170–178.
[6] M.-C. Wu, H.-C. Liao, Y.-C. Cho, G. Toth, Y.-F. Chen, W.-F. Su, K. Kordas, Photo-Kelvin probe force microscopy for photocatalytic performance characterization of single filament of TiO_2 nanofiber photocatalysts, Journal of Materials Chemistry A 1 (2013) 5715–5720.
[7] X. Zhang, J.H. Pan, A.J. Du, W. Fu, D.D. Sun, J.O. Leckie, Combination of one-dimensional TiO_2 nanowire photocatalytic oxidation with microfiltration for water treatment, Water Research 43 (2009) 1179–1186.
[8] C. Kormann, D.W. Bahnemann, M.R. Hoffmann, Preparation and characterization of quantum-size titanium-dioxide, Journal of Physical Chemistry 92 (1988) 5196–5201.

[9] H. Lin, C.P. Huang, W. Li, C. Ni, S.I. Shah, Y.-H. Tseng, Size dependency of nanocrystalline TiO_2 on its optical property and photocatalytic reactivity exemplified by 2-chlorophenol, Applied Catalysis B-Environmental 68 (2006) 1–11.
[10] M. Pelaez, N.T. Nolan, S.C. Pillai, M.K. Seery, P. Falaras, A.G. Kontos, P.S.M. Dunlop, J.W.J. Hamilton, J.A. Byrne, K. O'Shea, M.H. Entezari, D.D. Dionysiou, A review on the visible light active titanium dioxide photocatalysts for environmental applications, Applied Catalysis B-Environmental 125 (2012) 331–349.
[11] G. Zhang, G. Kim, W. Choi, Visible light driven photocatalysis mediated via ligand-to-metal charge transfer (LMCT): an alternative approach to solar activation of titania, Energy & Environmental Science 7 (2014) 954–966.
[12] L.G. Devi, R. Kavitha, A review on non metal ion doped titania for the photocatalytic degradation of organic pollutants under UV/solar light: Role of photogenerated charge carrier dynamics in enhancing the activity, Applied Catalysis B-Environmental 140 (2013) 559–587.
[13] S.H. Kang, S.-H. Choi, M.-S. Kang, J.-Y. Kim, H.-S. Kim, T. Hyeon, Y.-E. Sung, Nanorod-based dye-sensitized solar cells with improved charge collection efficiency, Advanced Materials 20 (2008) 54.
[14] S.H. Kang, J.-Y. Kim, Y. Kim, H.S. Kim, Y.-E. Sung, Surface modification of stretched TiO_2 nanotubes for solid-state dye-sensitized solar cells, Journal of Physical Chemistry C 111 (2007) 9614–9623.
[15] B. Oregan, M. Gratzel, A Low-Cost, High-Efficiency Solar-Cell Based on Dye-Sensitized Colloidal TiO_2 Films, Nature 353 (1991) 737–740.
[16] A. Kongkanand, K. Tvrdy, K. Takechi, M. Kuno, P.V. Kamat, Quantum dot solar cells. Tuning photoresponse through size and shape control of CdSe-TiO_2 architecture, Journal of the American Chemical Society 130 (2008) 4007–4015.
[17] I. Robel, V. Subramanian, M. Kuno, P.V. Kamat, Quantum dot solar cells. Harvesting light energy with CdSe nanocrystals molecularly linked to mesoscopic TiO_2 films, Journal of the American Chemical Society 128 (2006) 2385–2393.
[18] W.K. Ho, J.C. Yu, Sonochemical synthesis and visible light photocatalytic behavior of CdSe and CdSe/TiO_2 nanoparticles, Journal of Molecular Catalysis a-Chemical 247 (2006) 268–274.
[19] C.-S. Lim, M.-L. Chen, W.-C. Oh, Synthesis of CdSe-TiO_2 Photocatalyst and Their Enhanced Photocatalytic Activities under UV and Visible Light, Bulletin of the Korean Chemical Society 32 (2011) 1657–1661.
[20] J. Zhu, D. Yang, J. Geng, D. Chen, Z. Jiang, Synthesis and characterization of bamboo-like CdS/TiO_2 nanotubes composites with enhanced visible-light photocatalytic activity, Journal of Nanoparticle Research 10 (2008) 729–736.
[21] R. Brahimi, Y. Bessekhouad, A. Bouguelia, M. Trari, Improvement of eosin visible light degradation using PbS-sensititized TiO_2, Journal of Photochemistry and Photobiology a-Chemistry 194 (2008) 173–180.
[22] C. Wang, K.-W. Kwon, M.L. Odlyzko, B.H. Lee, M. Shim, PbSe nanocrystal/TiOx heterostructured films: A simple route to nanoscale heterointerfaces and photocatalysis, Journal of Physical Chemistry C 111 (2007) 11734–11741.
[23] J.-C. Lee, T.G. Kim, H.-J. Choi, Y.-M. Sung, Enhanced photochemical response of TiO_2/CdSe heterostructured nanowires, Crystal Growth & Design 7 (2007) 2588–2593.
[24] D. Liu, P.V. Kamat, Photoelectrochemical Behavior of Thin Cdse and Coupled TiO_2 CdSe Semiconductor-Films, Journal of Physical Chemistry 97 (1993) 10769–10773.
[25] L.M. Peter, D.J. Riley, E.J. Tull, K.G.U. Wijayantha, Photosensitization of nanocrystalline TiO_2 by self-assembled layers of CdS quantum dots, Chemical Communications (2002) 1030–1031.
[26] R. Vogel, K. Pohl, H. Weller, Sensitization of Highly Porous, Polycrystalline TiO_2 Electrodes by Quantum Sized Cds, Chemical Physics Letters 174 (1990) 241–246.
[27] Y.-S. Li, F.-L. Jiang, Q. Xiao, R. Li, K. Li, M.-F. Zhang, A.-Q. Zhang, S.-F. Sun, Y. Liu, Enhanced photocatalytic activities of TiO_2 nanocomposites doped with water-soluble mercapto-capped CdTe quantum dots, Applied Catalysis B-Environmental 101 (2010) 118–129.
[28] P. Yu, K. Zhu, A.G. Norman, S. Ferrere, A.J. Frank, A.J. Nozik, Nanocrystalline TiO_2 solar cells sensitized with InAs quantum dots, Journal of Physical Chemistry B 110 (2006) 25451–25454.
[29] A. Zaban, O.I. Micic, B.A. Gregg, A.J. Nozik, Photosensitization of nanoporous TiO_2 electrodes with InP quantum dots, Langmuir 14 (1998) 3153–3156.
[30] R. Plass, S. Pelet, J. Krueger, M. Gratzel, U. Bach, Quantum dot sensitization of organic-inorganic hybrid solar cells, Journal of Physical Chemistry B 106 (2002) 7578–7580.
[31] C. Ratanatawanate, C. Xiong, K.J. Balkus, Jr., Fabrication of PbS quantum dot doped TiO_2 nanotubes, Acs Nano 2 (2008) 1682–1688.
[32] K.P. Acharya, T.R. Alabi, N. Schmall, N.N. Hewa-Kasakarage, M. Kirsanova, A. Nemchinov, E. Khon, M. Zamkov, Linker-Free Modification of TiO_2 Nanorods with PbSe Nanocrystals, Journal of Physical Chemistry C 113 (2009) 19531–19535.
[33] R.D. Schaller, M. Sykora, J.M. Pietryga, V.I. Klimov, Seven excitons at a cost of one: Redefining the limits for conversion efficiency of photons into charge carriers, Nano Letters 6 (2006) 424–429.
[34] F.W. Wise, Lead salt quantum dots: The limit of strong quantum confinement, Accounts of Chemical Research 33 (2000) 773–780.
[35] W.W. Yu, J.C. Falkner, B.S. Shih, V.L. Colvin, Preparation and characterization of monodisperse PbSe semiconductor nanocrystals in a noncoordinating solvent, Chemistry of Materials 16 (2004) 3318–3322.
[36] E. Horvath, A. Kukovecz, Z. Konya, I. Kiricsi, Hydrothermal conversion of self-assembled titanate nanotubes into nanowires in a revolving autoclave, Chemistry of Materials 19 (2007) 927–931.
[37] A.C. Almeida Silva, S.L. Vieira de Deus, M.J. Barbosa Silva, N.O. Dantas, Highly stable luminescence of CdSe magic-sized quantum dots in HeLa cells, Sensors and Actuators B-Chemical 191 (2014) 108–114.
[38] X.B. Chen, A.C.S. Samia, Y.B. Lou, C. Burda, Investigation of the crystallization process in 2nm CdSe quantum dots, Journal of the American Chemical Society 127 (2005) 4372–4375.
[39] S.S. Narayanan, S.K. Pal, Aggregated CdS quantum dots: Host of biomolecular ligands, Journal of Physical Chemistry B 110 (2006) 24403–24409.
[40] S. Neeleshwar, C.L. Chen, C.B. Tsai, Y.Y. Chen, C.C. Chen, S.G. Shyu, M.S. Seehra, Size-dependent properties of CdSe quantum dots, Physical Review B 71 (2005).
[41] J.H. Yoon, W.S. Chae, S.J. Im, Y.R. Kim, Mild synthesis of ultra-small CdSe quantum dots in ethylenediamine solution, Materials Letters 59 (2005) 1430–1433.
[42] A. Sashchiuk, L. Langof, R. Chaim, E. Lifshitz, Synthesis and characterization of PbSe and PbSe/PbS core-shell colloidal nanocrystals, Journal of Crystal Growth 240 (2002) 431–438.
[43] C.M. Evans, L. Guo, J.J. Peterson, S. Maccagnano-Zacher, T.D. Krauss, Ultrabright PbSe magic-sized clusters, Nano Letters 8 (2008) 2896–2899.
[44] M. Qamar, C.R. Yoon, H.J. Oh, N.H. Lee, K. Park, D.H. Kim, K.S. Lee, W.J. Lee, S.J. Kim, Preparation and photocatalytic activity of nanotubes obtained from titanium dioxide, Catalysis Today 131 (2008) 3–14.
[45] M.-C. Wu, A. Sapi, A. Avila, M. Szabo, J. Hiltunen, M. Huuhtanen, G. Toth, A. Kukovecz, Z. Konya, R. Keiski, W.-F. Su, H. Jantunen, K. Kordas, Enhanced photocatalytic activity of TiO_2 nanofibers and their flexible composite films: Decomposition of organic dyes and efficient H-2 generation from ethanol-water mixtures, Nano Research 4 (2011) 360–369.
[46] K. Prabakar, S., Minkyu, S., Inyoung, K. Heeje, CdSe quantum dots co-sensitized TiO_2 photoelectrodes: particle size dependent properties, Journal of Physics D-Applied Physics, 43 (2010).
[47] M. Liangliang, J. Wuzhou, H. Lijuan, F. Pengfei, Photocatalytic Activity of TiO_2 Sensitized by CdS Quantum Dots under Visible-Light Irradiation, Wuhan University Journal of Natural Sciences 16 (2011) 313–318.